19 (2026) 100275

Contents lists available at ScienceDirect

Superconductivity

journal homepage: www.elsevier.com/locate/supcon

Rapid Letter

Breakdown strength of PPLP and kapton in liquid hydrogen and comparison with liquid nitrogen

Luhan Zu [a], Stéphane Holé [a,*], Nicolas Lallouet [b], Christoph Haberstroh [c], Johannes Doll [c], Adela Marian [d], Christian-Éric Bruzek [e]

[a] LPEM, ESPCI Paris PSL University, Sorbonne University, CNRS, Paris, France
[b] NEXANS, Calais, France
[c] Technical University Dresden, Dresden, Germany
[d] Research Institute for Sustainability at GFZ, Potsdam, Germany
[e] ASG Superconductors SpA, Genoa, Italy

ARTICLE INFO

Keywords:
High voltage superconducting cable
Liquid nitrogen (LN_2)
Liquid hydrogen (LH_2)
Insulation
Breakdown
PPLP
Kapton

ABSTRACT

Electricity transmission with superconducting cables uses various cooling media. Liquid hydrogen (LH_2) is well suited for magnesium diboride (MgB_2), but the breakdown strength of LH_2-impregnated insulation has not been tested yet. In this letter, polypropylene laminated paper (PPLP) and polyimide (Kapton) insulation structures are tested in the same conditions in LH_2 and LN_2 (liquid nitrogen). The results show that Kapton presents a similar behavior for both cooling media whereas PPLP exhibits a lower shape parameter, *i.e.* a broader breakdown event scattering, in LH_2 than in LN_2 though scale parameters, *i.e.* breakdown strength at 63% cumulative probability, are similar.

The decarbonization of large-scale energy transmission infrastructures has stimulated renewed interest in superconducting power cables cooled by cryogenic fluids [1]. Two technologies are considered, one using high temperature superconductors (HTS) [2] and one using low temperature superconductors (LTS) [3]. Though HTS seems more convenient since they can operate in liquid nitrogen (LN_2), they are crystals thus brittle and difficult to fabricate in long length resulting in high prices. On the contrary LTS are simple and robust materials easy to fabricate in long length, but they require a lower temperature to operate. With the discovery of MgB_2 and its critical transition temperature at 39 K [4], liquid hydrogen (LH_2) has become a convenient cryogenic fluid, since it is abundant and light. Within this context, LH_2 represents a strategic medium, combining cryogenic cooling capability with its potential role as a chemical energy carrier. The Horizon Europe SCARLET project (Superconducting CAbles foR sustainabLe Energy Transition) aims to develop high-power MgB_2-based superconducting cables operating in liquid hydrogen environments [5]. As transporting large quantities of electric power requires both current and voltage, a critical challenge in this framework concerns the dielectric reliability of the insulating structures impregnated by LH_2 under high continuous (dc) electric stress. At low temperatures, solid materials cannot be used for the insulation because their expansion coefficient is too different from the conductor one. This would result in cracks during or after cooling. Therefore tapes are used instead to allow cable flexibility and thermal expansion compliance. In order to size the cable insulation and assess risk management, it is mandatory to test the breakdown strength of the insulating structure. While insulation impregnated with LN_2 has been extensively investigated over the past decades, including under hydrostatic pressure and for various geometries [6–11], the breakdown strength in LH_2 impregnated structures remains unexplored so far. The distinct thermophysical properties of LH_2 may however significantly influence breakdown mechanisms compared to LN_2. Nevertheless, systematic datasets remain mostly non-existent owing to the intrinsic experimental complexity mainly due to safety concerns associated with the use of LH_2.

Previous work within the SCARLET project has addressed the breakdown performance in LN_2, including statistical methodology development and comparison between different lapped insulation structures arranged for being representative of a real superconducting cable geometry [10,11]. If the tape material and the cryogenic fluid greatly contribute to the efficiency of the insulation, the adopted geometry has also a great influence. For instance a smaller butt-gap improves breakdown strength [11], but this is at the expense of the cable flexibility. Therefore, both material and representative structure must be tested for cable application. The present contribution extends the work in LN_2 to LH_2 and focuses exclusively on the comparison between LH_2 and LN_2 break-

* Corresponding author.
E-mail address: stephane.hole@espci.fr (S. Holé).

https://doi.org/10.1016/j.supcon.2026.100275
Received 12 May 2026; Received in revised form 2 July 2026; Accepted 11 July 2026
Available online 13 July 2026

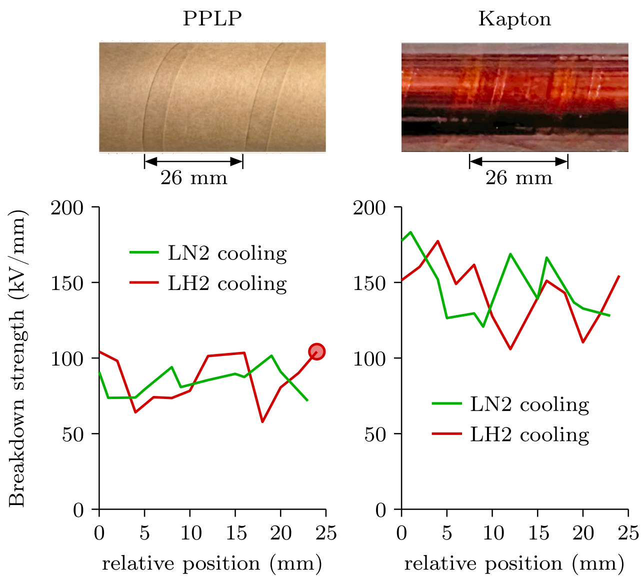

Fig. 1. Sample structure (top) and breakdown field strength along one sample period (bottom) for PPLP samples (left) and Kapton samples (right). The closed circle (bottom left) corresponds to a test that did not result in a breakdown.

down performances for the representative cable insulation geometry of SCARLET project.

The tested samples consisted of 4 layers of 168-μm-thick polypropylene laminated paper (PPLP) insulation and 5 layers of 50-μm-thick polyimide (Kapton) insulation. They were prepared to reproduce the composite configuration of a practical cable insulation. For this purpose, each sample was mounted on a 27-mm-diameter 70-cm-long metallic cylinder acting as the high-voltage positive electrode. The insulation tapes, 20 mm in width, were wound onto this metallic cylinder such that butt-gaps were about 4 mm. The number of layers was limited to its minimum to still show the same density of insulation tapes and gaps underneath compared to thicker structures and reduce the required maximum voltage to trigger a breakdown. The butt-gaps are important for cable flexibility, therefore the lapped architecture intentionally introduces alternating regions of solid polymer and cryogenic fluid. One spatial period is shown for PPLP and Kapton samples in the top of Fig. 1. The length of the insulation period along the sample axis is about 26 mm considering the tape tilt on the cylinder.

A grounded electrode rolling on the surface of the insulation ensured localized breakdown initiation at controlled positions along the sample. After each breakdown event, the electrode position was displaced by 12 mm in LH_2 and 15 mm in LN_2 in order to ensure statistical independence between successive tests and to scan evenly all positions of the period of the insulation lapping with about 2 mm accuracy (see Supplementary Material). This procedure enables multiple breakdown acquisitions under almost identical thermodynamic conditions within a single cooling cycle, thereby minimizing variability.

While cooling and performing breakdown tests in LN_2 present no difficulty, it is not the case in LH_2 owing to safety concerns. Therefore, a preliminary cooling with cold helium gas (GHe) was done. In addition to cooling down the inner part of the cryostat to about 20 K, which corresponds to LH_2 temperature, it makes it possible to check the good operation of the test bench at LH_2 temperature and to locate leakages with an helium detector prior to transferring LH_2. Meanwhile, all electrical devices were enclosed in a box over-pressurized with nitrogen gas (GN_2) in order to prevent the risk of ignition in presence of hydrogen at all times during the tests. While the exhaust of GHe during pre-cooling was recycled, the exhausts of nitrogen and hydrogen from the boil-off during the tests were released in the atmosphere at a sufficient height for safety. After the tests, LN_2 or LH_2 were transferred back to their Dewar and the cryostat was slowly warmed up using room temperature GN_2.

Breakdown tests were conducted in LN_2 and LH_2 at near-atmospheric pressure in boiling conditions (1007 ± 7 mbar). The positive dc voltage was increased at a rate of 200 V/s until the breakdown occurrence. Twelve breakdown events were recorded for each material and cooling medium. As samples have not the same thickness, the nominal electric field strength, corresponding to the breakdown voltage divided by the overall insulation thickness, is used in the presented results. Raw breakdown voltage measurements can be found in Supplementary Material. Although the composite insulating structure contains both solid and fluid-filled parts, and thus a non uniform electric field, this normalization reflects the macroscopic electric stress experienced in real cable insulation systems since the same voltage is applied along the cable regardless the insulating structure between the electrodes. The graphs in the bottom of Fig. 1 do not seem to show strong patterns relative to the sample structure. Since breakdown tests were performed at evenly distributed positions in the sample period, the dataset is therefore well representative of the insulation in its whole.

The cumulative probability (CDF) of breakdown was modeled according to the two-parameter Weibull distribution [12–14]. The scale parameter α corresponds to the breakdown electric field strength at 63% cumulative probability and represents the characteristic dielectric strength of the insulation system. The shape parameter β describes the dispersion of breakdown events and governs the steepness of the cumulative probability curve. Weibull parameters are generally estimated with Bernard's law [13] with more than 12 points to minimize errors in the empirical CDF estimation. However, the linear fit required in that case relies on the extreme points of the distribution that are of much lower probability. Therefore the Weibull parameters reported in this letter were obtained by the maximum likelihood estimation (MLE) [15]. Bernard's law is used only to plot the experimental points graphically in the usual Weibull diagrams. Confidence regions for the scale and shape parameters were evaluated to assess statistical significance of observed differences between LN_2 and LH_2. The variability of the estimations, indicated in parentheses thereafter, is the maximal value calculated with the leave-one-out method [16].

During testing, only one test did not result in a breakdown because the applied voltage reached the maximum voltage of the supply, which is 70 kV. This event was therefore not taken into account in the estimation of α and β with MLE but it is indicated graphically in the Weibull diagram for completeness of CDF according to Bernard's law. As its horizontal position is meaningless (this is the maximum voltage of the supply), the parameter calculation with this event would have resulted in an underestimation of α and an overestimation of β.

Results for PPLP (Fig. 2) lead to a scale parameter α = 88.9 kV/mm (+1.0/ − 2.1) and a shape parameter β = 10.6 (+2.8/ − 0.6) when impregnated with LN_2 and α = 90.6 kV/mm (+2.1/ − 2.1) and β = 6.4 (+1.0/ − 0.4) when impregnated with LH_2. Though the scale parameter α seems slightly larger in LH_2 than in LN_2, the shape parameter β is significantly smaller in LH_2 than in LN_2. It can be said that breakdown strength is scaled the same way (similar α) for both cryogenic fluids whereas breakdown events are broaderly distributed (smaller β) for LH_2. Therefore, at low breakdown probability, cables with LH_2 impregnation fluid have higher insulation requirements. This can be mitigated by the fact that numerous breakdowns occurred well above those in LN_2 and other well below. A plausible hypothesis to try to explain the larger shape parameter β in LH_2 is the fact that bubbles are a well known factor of breakdown in liquids [17]. Indeed, LH_2 has a latent heat of evaporation of 31.7 J/cm^3 well below the one of LN_2 of 160.8 J/cm^3, leading to an easier appearance of bubbles in LH_2 than in LN_2. Therefore, it can be assumed that a small energy input, for instance from an early partial discharge, is sufficient to generate bubbles that can trigger a breakdown at lower voltage in LH_2 than in LN_2. Also, It can be assumed that a larger presence of gaps at the breakdown position gives more room for bubble enlargement and thus increases breakdown

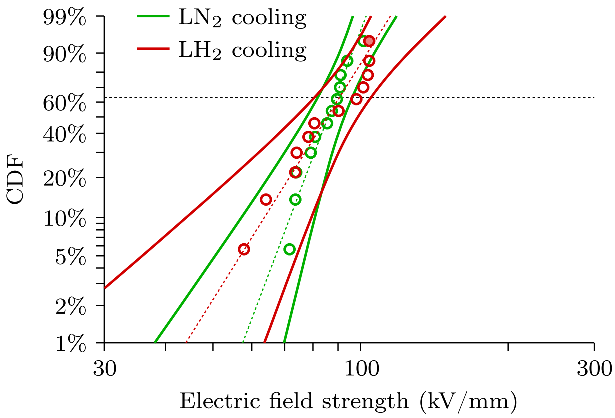

Fig. 2. Weibull representation of breakdown electric field strength for PPLP insulation in LN_2 and LH_2 under identical voltage ramps and experimental conditions. Open circles correspond to the measured breakdowns, dotted lines correspond to the estimated Weibull parameters and continuous lines correspond to 95% confidence. The closed circle is a test that did not result in a breakdown.

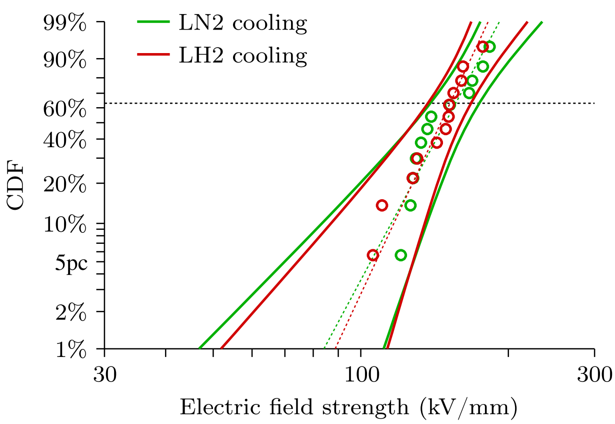

Fig. 3. Weibull representation of breakdown electric field strength for Kapton insulation in LN2 and LH2 under identical voltage ramps and experimental conditions. Open circles correspond to the measured breakdowns, dotted lines correspond to the estimated Weibull parameters and continuous lines correspond to 95% confidence.

probability. This effect is further accentuated by a larger coefficient between liquid and gas densities for hydrogen than for nitrogen.

Results for Kapton (Fig. 3) lead to a scale parameter $\alpha = 156.2$ kV/mm (+2.1/ − 4.2) and a shape parameter $\beta = 7.4$ (+0.5/ − 0.4) when impregnated with LN_2 and $\alpha = 152.2$ kV/mm (+2.4/ − 4.0) and $\beta = 8.5$ (+1.7/ − 0.5) when impregnated with LH_2. In contrast to PPLP, both results are very similar indicating a low influence of the cooling medium. This can be interpreted with the difference in layer thickness of the two materials. Indeed, a smaller layer thickness implies a smaller gap volume, thus less fluid to vaporize, here the volume in Kapton gaps is smaller than one third of the one in PPLP gaps.

In conclusion, though the scale parameter as well as many breakdown voltages are larger in LH_2 than in LN_2 for PPLP, the shape parameter is significantly lower in LH_2. Therefore the reduction of breakdown probability in LH_2 involves more PPLP layers than in LN_2 for the insulation. By contrast, Kapton insulation exhibits nearly identical Weibull parameters in LN_2 and LH_2. The assumptions to explain this behavior are an easier bubble generation in LH_2 than in LN_2 and a smaller volume in the gaps for thinner tapes (Kapton) than for thicker tapes (PPLP). Choosing the right material depends on the application constraints. Based on this study, PPLP should be chosen for cable insulation due to their lower price even if it is at the expense of a thicker insulation.

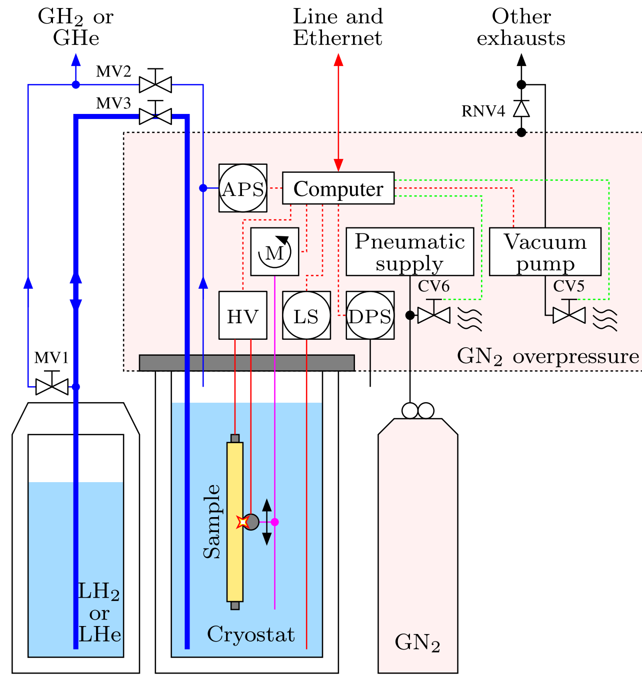

Fig. 4. Sketch of LH_2 setup. All electronics are enclosed in a pressurized (20 mbar) GN_2 box (in light pink). The computer is controlled remotely via a web interface through Ethernet. This computer monitors and controls the various devices, sensors and valves (APS stands for absolute pressure sensor, DPS for differential pressure sensor, LS for level sensor, HV for high voltage supply, M for motor, MV for manual valves, RNV for non-return valve and CV for controlled valves).

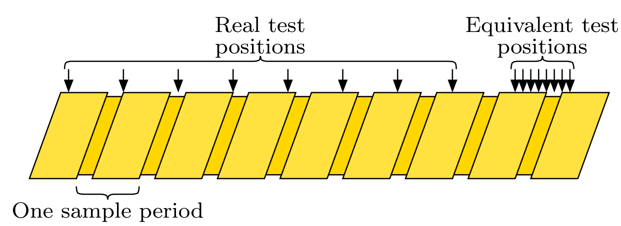

Fig. 5. Illustration of test under-sampling. In this illustration, tests are performed every 7/8 of the sample period. Therefore the sample structure is completely tested after 8 measurements with an equivalent resolution of 1/8 of the sample period.

On the contrary Kapton should be chosen if compactness is important. Further work is however necessary to optimize the insulation geometry, for instance to reduce butt-gap size wile keeping flexibility, and test breakdown strength under hydrostatic pressure.

Supplementary material

The set-up, sketched in Fig. 4, was cooled down to a temperature lower than 20 K using helium gas (GHe) from a liquid helium (LHe) Dewar. GHe exhausts was recycled. During cooling, leakages were detected using an ASM detector from Pfeiffer and then fixed to continue the experiment. Once the cryostat sufficiently cold, liquid hydrogen (LH_2) was transferred to the cryostat and hydrogen exhaust was released in the atmosphere. At the end of the transfer, valves MV1 and MV2 were left open while MV3 was closed to maintain boiling conditions under atmospheric pressure in the cryostat. The pressure was controlled by a DPI-104 from Druck and remained stable at 1007 ± 7 mbar absolute pressure.

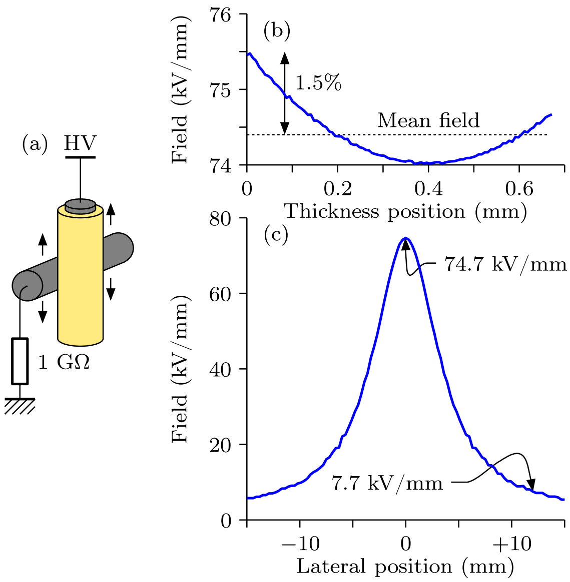

Fig. 6. Electric field calculated by finite element method at breakdown point. (a) sketch of the arrangement of the rolling cylinder on the sample. (b) Electric field strength from the inner electrode to the rolling cylinder. (c) Electric field strength along the inner electrode.

Table 1
Breakdown voltages in kilovolt (kV) for PPLP and Kapton structures impregnated with liquid nitrogen (LN2) or liquid hydrogen (LH2). The underlined value corresponds to a test that did not result in a breakdown.

Breakdown voltage in kV			
PPLP		Kapton	
LN2	LH2	LN2	LH2
61.03	70.00	44.40	37.87
60.15	68.10	34.80	26.48
49.68	70.02	38.00	38.65
68.22	52.61	34.20	31.91
63.15	60.60	32.40	32.59
48.14	49.45	32.00	40.42
57.45	54.10	42.20	27.62
49.47	49.78	45.80	37.26
58.74	38.86	41.60	35.75
53.22	43.11	31.60	44.34
61.17	69.52	33.20	37.77
54.32	65.93	30.20	40.09

The measurements began with the rolling electrode at the highest position. For each test, the high voltage supply (HV in Fig. 4, HPp-700-505 from ISEG) ramped up at 200 V/s, from about 10 kV. The inner electrode of the sample is positively polarized. When breakdown occurred, the supply automatically switched off thanks to the Kill mode. Data from sensors were recorded every seconds and stored to a file. After each breakdown test, the rolling electrode was shifted down by 12 or 15 mm depending on the sample in order to obtain 2-mm equivalent spatial resolution in the insulation period (see Fig. 5). After all measurements, LH_2 was transferred back to its Dewar by closing MV2 and opening MV1 and MV3. Finally the Dewar was stored and the cryostat was gently warmed up with room temperature nitrogen gas (GN_2) during one night.

The test point is realized between two perpendicular cylinders. One of the cylinder is the sample inner electrode with its 27-mm diameter, the other cylinder is a rolling electrode connected to ground through a 1-GΩ resistor as sketched in Fig. 6a. Fig. 6b and c show the electric field amplitude between the electrodes and along the inner electrode respectively. This shows that the electrode geometry deforms the electric field uniformity less than 2% and that the electric field is well localized along the sample surface since it is divided by almost 10 at 12 mm from the test point.

Table 1 reports the raw breakdown voltages measured in PPLP and Kapton impregnated with liquid nitrogen (LN_2) or liquid hydrogen (LH_2). The overall thickness of the PPLP sample is 672 μm and the overall thickness of Kapton is 250 μm.

CRediT authorship contribution statement

Luhan Zu: Writing – original draft, Software, Methodology, Investigation, Formal analysis, Data curation, Conceptualization; **Stéphane Holé:** Writing – review & editing, Validation, Supervision, Methodology, Investigation, Formal analysis, Data curation, Conceptualization; **Nicolas Lallouet:** Resources; **Christoph Haberstroh:** Writing – review & editing, Resources; **Johannes Doll:** Resources; **Adela Marian:** Writing – review & editing, Project administration; **Christian-Éric Bruzek:** Writing – review & editing, Supervision, Project administration.

Declaration of competing interest

The authors declare that they have no known competing financial interests or personal relationships that could have appeared to influence the work reported in this paper.

Acknowledgements

This project has received funding from the European Union's Horizon Europe research and innovation program under grant agreement No 101075602. The authors want to thank Max Grabowski, Thomas Just and Marcus Dietzel for their support in the lab during the LH2 tests.

References

[1] Buchholz A, Noe M, Kottonau D, Shabagin E, Weil M. Environmental life-cycle assessment of a 10 kv high-temperature superconducting cable system for energy distribution. IEEE Trans Appl Supercond 2021;31:1–5. https://doi.org/10.1109/tasc.2021.3070703
[2] Honjo S, Mimura T, Kitoh Y, Noguchi Y, Masuda T, Yumura H, et al. Status of superconducting cable demonstration project in Japan. IEEE Trans Appl Supercond 2011;21:967–71. https://doi.org/10.1109/tasc.2010.2092744
[3] Savoldi L, Balbo A, Bruzek CE, Grasso G, Patti M, Tropeano M. Conceptual design of a superconducting energy pipeline for LH2 and power transmission over long distances. IEEE Trans Appl Supercond 2024;34:3370123. https://doi.org/10.1109/tasc.2024.3370123
[4] Nagamatsu J, Nakagawa N, Muranaka T, Zenitani Y, Akimitsu J. Superconductivity at 39 k in magnesium diboride. Nature 2001;410(6824):63–4. https://doi.org/10.1038/35065039
[5] Superconducting cables for sustainable energy transition (scarlet). 2022. https://scarlet-project.eu/project/.
[6] Pierrat L, Montanari GC, Mazzanti G, Cacciari M. Weibull statistics in short-term dielectric breakdown of thin polyethylene films [comments and reply]. IEEE Trans Dielectr Electr Insul 1995;2(2):321–6. https://doi.org/10.1109/94.388259
[7] Seong J-K, Seo I-J, Hwang J-S, Lee B-W. Comparative evaluation between DC and AC breakdown characteristic of dielectric insulating materials in liquid nitrogen. IEEE Trans Appl Supercond 2012;22(3):7701504. https://doi.org/10.1109/tasc.2011.2178222
[8] Andersen A, Dennison JR. Mixed Weibull distribution model of DC dielectric breakdowns with dual defect modes. In: 2015 IEEE conference on electrical insulation and dielectric phenomena (CEIDP). IEEE; 2015, p. 570–3. https://doi.org/10.1109/ceidp.2015.7352017
[9] Li C, Zhang F, Liu K, Luo S, Chen N, Zhang J, et al. Partial discharge behaviors of surface modified polyimide films in liquid nitrogen. In: 2018 IEEE International conference on applied superconductivity and electromagnetic devices (ASEMD). IEEE; 2018, p. 1–2. https://doi.org/10.1109/asemd.2018.8558940
[10] Zu L, Holé S, Bruzek C-É, Gamper G, Melaccio U, Lallouet N. Constant voltage breakdown measurement of lapped insulation under cryogenic conditions. In: Proceedings of the 2024 IEEE 5th international conference on dielectrics (ICD 2024). Toulouse, France: IEEE; 2024, p. 1–4. https://doi.org/10.1109/ICD59037.2024.10613052
[11] Zu L, Holé S, Lallouet N, Gamper G, Bruzek C-É. Breakdown field strength of lapped Kraft paper, PPLP, or Kapton in liquid nitrogen. IEEE Trans Dielectr Electr Insul 2025;32(6):3727–35. https://doi.org/10.1109/TDEI.2025.3619463
[12] Dissado LA, Fothergill JC, Wolfe SV, Hill RM. Weibull statistics in dielectric breakdown; theoretical basis, applications and implications. IEEE Trans Electr Insul 1984;EI-19:227–33. https://doi.org/10.1109/TEI.1984.298753

[13] Fothergill JC. Estimating the cumulative probability of failure data points to be plotted on Weibull and other probability paper. IEEE Trans Electr Insul 1990;25:489–92. https://doi.org/10.1109/14.55721

[14] Monsieur F, Vincent E, Roy D, Bruyère S, Pananakakis G, Ghibaudo G. Determination of dielectric breakdown Weibull distribution parameters confidence bounds for accurate ultrathin oxide reliability predictions. Microelectron Reliab 2001;41(9–10):1295–300. https://doi.org/10.1016/S0026-2714(01)00183-4

[15] Mohd Ikbal NA, Abdul Halim S, Ali N. Estimating Weibull parameters using maximum likelihood estimation and ordinary least squares: simulation study and application on meteorological data. Math Stat 2022;10:269–92. https://doi.org/10.13189/ms.2022.100201

[16] Smola AJ, Bartlett P, Schölkopf B, Schuurmans D, editors. IV. Leave-one-out methods. the MIT Press; 2000, https://doi.org/10.7551/mitpress/1113.001.0001

[17] Hill N, Kurrat M. Discharge mechanisms in liquid nitrogen-breakdown field strength of gaseous nitrogen. IEEE Trans Appl Supercond 2018;28. https://doi.org/10.1109/TASC.2018.2809460